Published in final edited form as:
Ann Neurol. 2014 June ; 75(6): 837–850. doi:10.1002/ana.24139.

Gp120 in the pathogenesis of human HIV-associated pain

Subo Yuan, MD, PhD[1,*], **Yuqiang Shi, PhD**[1,*], **Jinghong Chen, PhD**[2], **Xiangfu Zhou**[3], **Guangyu Li, PhD**[2], **Benjamin B. Gelman, MD, PhD**[4], **Joshua G. Lisinicchia, PhD**[4], **Susan M. Carlton, PhD**[1], **Monique R. Ferguson, PhD**[2], **Alai Tan. MD, PhD**[5], **Sushil K. Sarna, PhD**[2], and **Shao-Jun Tang, PhD**[1,#]

[1] Department of Neuroscience and Cell Biology, University of Texas Medical Branch, Galveston, Texas 77555

[2] Department of Internal Medicine, University of Texas Medical Branch, Galveston, Texas 77555

[3] Department of Urology, The Third Affiliated Hospital, Sun Yat-Sen University Guangzhou 510630, China

[4] Department of Pathology, The University of Texas Medical Branch, Galveston, Texas 77555

[5] Department of Preventive Medicine and Community Health, University of Texas Medical Branch, Galveston, Texas 77555

Abstract

Objective—Chronic pain is a common neurological comorbidity of HIV-1 infection, but the etiological cause remains elusive. The objective of this study was to identify the HIV-1 causal factor that critically contributes to the pathogenesis of HIV-associated pain.

Methods—We first compared the levels of HIV-1 proteins in postmortem tissues of the spinal cord dorsal horn (SDH) from HIV-1/AIDS patients who developed chronic pain (‘pain-positive’ HIV-1 patients) and HIV-1 patients who did not develop chronic pain (‘pain-negative’ HIV-1 patients). Then, we used the HIV-1 protein that was specifically increased in the ‘pain-positive’ patients to generate mouse models. Finally, we performed comparative analyses on the pathological changes in the models and the HIV-1 patients.

Results—We found that HIV-1 gp120 was significantly higher in ‘pain-positive’ HIV-1 patients (vs. ‘pain-negative’ HIV-1 patients). This finding suggested that gp120 was a potential causal factor of the HIV-associated pain. To test this hypothesis, we used a mouse model generated by intrathecal injection (i.t.) of gp120 and compared the pathologies of the model and the ‘pain-positive’ human HIV-1 patients. The results showed that the mouse model and ‘pain-positive’ human HIV-1 patients developed extensive similarities in their pathological phenotypes, including pain behaviors, peripheral neuropathy, glial reactivation, synapse degeneration and aberrant activation of pain-related signaling pathways in the SDH.

[#] Corresponding author. Address correspondence to: Shao-Jun Tang, Ph.D., Department of Neuroscience and Cell Biology, University of Texas Medical Branch, Galveston, TX 77555-1069; Tel: 409-772-1190; shtang@utmb.edu.
[*]Co-first authors

Conflict of interest: None

Interpretation—Our findings suggest that gp120 may critically contribute to the pathogenesis of HIV-associated pain.

INTRODUCTION

HIV-1 infection is associated with a spectrum of neurological disorders that disturb the senosory, motor and cognitive functions HIV-1/AIDS patients [1]. These HIV-associated neurological disorders (neuroAIDS) often remain significantly prevalent even after highly active anti-retroviral treatment (HAART). Chronic pain is one of the most common neuroAIDS, affecting over 60% of HIV-1-infected patients [2-4]. Patients with the HIV-associated pain syndromes may suffer headache, somatic pain and visceral pain [2-5]. Chronic pain dramatically deteriorates the quality of life of HIV-1/AIDS patients and is one of the primary reasons for them to seek medical assistance. Concomitant with pain manifestation, about 30% of HIV-1/AIDS patients develop clinically detectable peripheral neuropathy[6]. These neuropathological findings show that HIV-1 infection impairs the pain transmission pathways. Clinical interventions currently available provide only symptomatic relief, rather than a cure. The understanding of how HIV-1 infection leads to chronic pain is essential for the development of effective therapy.

To elucidate the pathogenic mechanism of HIV-associated pain, it is critical to identify the causative HIV-1 agents. Several HIV-1 proteins have been shown to induce pain behaviors when introduced into animal models. The tested HIV-1 proteins include gp120 [7-14] and Vpr [15]. Some models were created by exposing either the sciatic nerve [7, 9, 13, 14, 16] or the spinal cord [8, 10] to HIV-1 proteins. Others were created by transgenic expression of HIV-1 proteins [12, 15]. Gp120 can cause axonal injury of sensory neurons in culture [17-19]. Together with antiretroviral drugs, gp120 also induce cutaneous denervation in the transgenic mouse model [12] and in the sciatic nerve exposure model [7, 13]. *In vitro* studies suggest that HIV-1 trans-activator of transcription (Tat) can also stimulate sensory neurons in culture [20]. Although these studies suggest the sufficiency of multiple HIV-1 proteins in causing pain pathology in animals, the relevance of these proteins to the HIV-associated pain in human patients is unclear. We currently lack HIV-1 patient-based studies that can establish the etiological relevance of any HIV-1 protein. This caveat presents a significant barrier to the mechanistic understanding of HIV-associated pain

To address this deficiency, we have compared HIV-1 proteins in the spinal cord dorsal horn (SDH) of the ‘pain-positive’ and ‘pain-negative’ HIV-1 patients. We found that HIV-1 gp120 was approximately 10 fold higher in the SDH of the ‘pain-positive’ HIV-1 patients than in the ‘pain-negative’ HIV-1 patients. To further test the relevance of gp120, we administered gp120 perispinally in mice via intrathecal injection (i.t.) and compared the pathological phenotypes of this mouse model with the pathologies in HIV-1 human patients. The results revealed extensive pathological similarities, at the behavioral, neurological, glial, synaptic and molecular levels, between the mouse model and the ‘pain-positive’ HIV-1 patients. Our findings provide evidence for the relevance of gp120 in causing HIV-associated pain.

MATERIALS AND METHODS

Animals

Adult C57Bl6 mice (female, 18-23g) and adult Sprague-Dawley rats (160-230g) were used. Animals were housed in cages with soft bedding under a 12 hr-reverse light/dark cycle. Animal procedures were performed following protocols that were reviewed and approved by the University of Texas Medical Branch Animal Care and Use Committee. Every attempt was made to reduce the number of animals used in these studies.

Materials

HIV-1 gp120 protein (HIV-1 $gp120_{IIIB}$, Cat # 11784; $gp120_{Bal}$, Cat # 4961) and antibodies against HIV-1 proteins were obtained through the NIH AIDS Research and Reference Reagent Program, Division of AIDS, NIAID, NIH. Antibodies for immunoblotting: anti-HIV-1 gp120 antibody (1:1000, Cat # 4091), anti-HIV-1 Tat (1:1000, Cat # 4672), anti-HIV-1 P24 (1:500, Cat # 6458) and anti-HIV-1 Vpr (1:500, Cat # 11836), anti-GFAP (1:5000, Cat # 04-1062, Millipore), anti-Iba1 (1:2000, Cat # 016-20001, Wako), anti-TNFα (1:1000, Cat # ab1793, Abcam), anti-IL-1β (1:1000, Cat # sc-7884, Santa Cruz), anti-PSD95 (1:2000, Cat # 2507, Cell Signaling), anti-Synapsin I (1:2000, Cat # AB1543, Millipore), anti-NR1 (1:2000, Cat # 06-311, Millipore), anti-phospho JNK (1:1000, Cat # 9251, Cell Signaling), anti-phospho-ERK1/2 (1:1000, Cat # 4370, Cell Signaling), anti-phospho-CaMKIIα (1:1000, Cat # sc-12886-R, Santa Cruz) and anti-β-actin (1:1000, Cat # sc-1616-R, Santa Cruz). Antibody for fluorescent immunostaining: anti-PGP 9.5 (1:500, Cat # 7863-0504, AbD). Antibody for DAB staining: anti-PGP9.5 (1:4000, Cat # AB1761, Millipore).

Human postmortem tissues

Fifteen human patients were selected from the autopsy archive of the Texas NeuroAIDS Research Center, which is one unit of The National NeuroAIDS Tissue Consortium (NNTC) [21]. The patients included three groups that were age-matched males (average ages: ~43 years), and the detailed patient information was previously described [22]. Group 1 (#1-5) consisted of five HIV-1 seronegative subjects, with no known history of peripheral neuropathy, myelopathy or chronic pain (HIV^- $Pain^-$). Group 2 (#6-10) consisted of five HIV-positive subjects with no clinically evident HIV-associated distal sensory neuropathy (HDSPN), clinical or neuropathological myelopathy, or clinical pain syndrome (i.e. 'pain-negative' HIV patients; HIV^+ $Pain^-$). Group 3 (#11-15) consisted of five HIV-positive subjects with HDSPN and clinically documented pain syndrome (i.e. 'pain-positive' HIV patients; HIV^+ $Pain^+$). For all 15 subjects, complete autopsies were performed, including the diagnosis of peripheral neuropathy in postmortem sural nerve biopsies. The spinal cord tissues were sectioned into 1.0 mm slices and stored at -80°C.

Gp120 intrathecal injection (i.t.)

Mice or rats were initially anaesthetized by inhaling 3% isoflurane. After the animals were sedated for 1-2 min, the isoflurane concentration was reduced to 2.5%. For mice, a 30½ gauge stainless-steel needle attached to a 10 μl luer tip syringe (Hamilton, Reno, NV) was

used for i.t. injections. To perform the i.t. injection, the experimenter used the left index finger to locate the intervertebral space between L5 and L6, and used the right hand to insert the syringe needle into the intervertebral space from a 45° angle. A correct intrathecal placement of the needle tip was judged by a tail twitch [23]. Gp120 protein was dissolved with 0.1% bovine serum albumin (BSA) in 0.1 M phosphate buffered saline (PBS) at a final concentration of 15ng/μl, and 7 μl of gp120 solution was injected. For i.t. injections in rats, 20 μl of the gp120 (300 ng) solution was administered with a 27G1¼ needle attached to 50 μl Luer tip syringe (Hamilton, Reno. Nevada).

Measurement of mechanical sensitivity

Paw withdrawal thresholds (PWT) were measured by von Frey testing on the plantar surface of the hind paw. Prior to testing, mice were habituated to the testing surroundings, by restraining them in a 5¼ × 2 × 1¾″ plexi-glass box on a metal mesh floor for one hour per day in three consecutive days. On the testing day, mice were first restrained in the plexi-glass box for 15 minutes. Then, calibrated von Frey filaments (Stoelting, Wood Dale, IL) were applied perpendicularly to the central area of the hind paw (when the hind paw plantar surface was flat on the metal mesh floor) until the filament started to bend. Positive nocifensive responses were counted when the behaviors of vertical or horizontal withdrawing, shaking, lifting, licking and/or biting the stimulated paw were observed. The animals were allowed to completely recover before the next test. Testing was done only when the animal was in a resting and alert state, avoiding the states when the animal was sleeping, exploring or grooming [24]. The experimenter was blinded to the treatment of each animal. The PWT was determined using the Dixon up/down method and plotted with GraphPad Prism 5 (mean ± SEM).

Measurement of visceromotor response to colorectal distension

Visceral hypersensitivity in rats was recorded by electromyographical (EMG) measurements of the visceromotor response (VMR) to colorectal distention (CRD) as previously reported [25]. Bipolar electrodes were implanted in the external oblique abdominal muscle and exteriorized in the subscapular region in rats under general anesthesia with 2.5% isoflurane inhalant. One week post-surgery, again under transient anesthesia with 2.5% isoflurane, a balloon (5 cm) made from a latex surgical glove finger connected to a length of Tygon tubing was placed inside the descending colon and rectum via the anus and held in place with tape to the tail. Rats were placed in Lucite cubicles (11×3 2/4 ×3 2/4″) to adapt for 30 min. On recovery from anesthesia, CRD was applied by steadily inflating the balloon to constant pressure with a sphygmomanometer linked to a pressure transducer. The balloon was inflated to graded pressures (10, 20, 40, 60 and 80 mm Hg) for a 20s duration, with a 2-min interval between tests. EMG signals were recorded on a Biopac System EMG 100 C (Biopac Systems Inc., Goleta, CA, USA). EMG signals were amplified (5000X), filtered with a 1-Hz high-pass filter, a 500-Hz low-pass filter and digitized using Acknowledge (Biopac Systems, Inc.). To define the area under the curve (AUC) for each distension period, the difference between integrals of the curve 20s before and after the distension period was calculated.

Immunohistochemistry staining

Mice were anaesthetized with ketamine (80 mg/kg) and xylazine (5 mg/kg) and transcardially perfused with PBS containing heparin (1000 unit/ml), followed with ice-cold fixative solution (4% paraformaldehyde in 0.1M PB). The glabrous skin biopsies were excised from the plantar area of the hind paw. The skin was kept in the same fixative at 4°C overnight and then in 30% sucrose/0.1 M PB for 48 hr. The skin biopsies were imbedded in optimum cryostat temperature (OCT) mounting medium (Sakura Finetek, USA) and frozen in methylbutane on dry ice/100% alcohol bath. Sagittal cryostat sections (14 μm) of hind paw skin were cut and mounted on glass slides pre-coated with poly-L-Lysine (Fisher).

For fluorescent immunostaining, sections were blocked with 5% bovine serum albumin (BSA) in 0.1M PBS with 0.3% Triton X-100. The sections were immunostained with rabbit anti-PGP9.5 antibody (AbD; 1:500 diluted with 2.5% BSA/0.1M PBS with 0.3% Triton X-100. The secondary antibody was goat anti-rabbit Alexa 488 (Invitrogen) diluted at 1:250 in the same antibody diluent. Stained sections were mounted with Vecta-Shield with DAPI (Vector). All digital images were obtained using a Bio-Rad Radiance Confocal microscope coupled to a Nikon E800 camera with Lasersharp 2000 imaging software.

For diaminobenzidine (DAB) staining, sections were blocked with the buffer as used in immunofluorescent staining. Rabbit anti-PGP9.5 antibody (Millipore, 1:4000) and biotinylated goat anti-rabbit secondary antibody (Vector, 5 μg/ml) were used. DAB staining was done with the ABC system (Vector). Sections were counter-stained with hematoxylin and mounted with Acrymount (StatLab). Digital images were obtained using an Olympus BX51 microscope.

Intraepidermal nerve fiber density

To determine the intraepidermal nerve fiber density (IENF) in the plantar area of the hind paw, PGP9.5-positive fibers in randomly selected areas along the junction between dermis and epidermis were imaged (60x magnification). IENF quantification was performed as described[12]. Fibers penetrating the dermis/epidermis junction were counted. Images from 5-6 animals were included for each group. For each animal, 8 glabrous sections were included in staining and 5 images of randomly picked areas along the epidermis/dermis junction were obtained from each section for IENF quantification.

Western blotting analysis

The lumbar SDH of human postmortem cases and mouse spinal cords were dissected out and homogenized in RIPA lysis buffer (1% Nonidet P-40, 50 mM Tris-HCl, 0.25% Na-deoxycholate, 150 mM NaCl, 1 mM EDTA, pH 7.4) containing a protease inhibitor cocktail (Sigma). After centrifugation (12,000g; 10 min), the supernatant was collected and the protein concentration was determined using the BCA Protein Assay Kit (Pierce). Equal amounts of protein (50 μg) were separated on SDS-PAGE gels, followed by transfer to Polyvinylidene fluoride (PVDF) membranes. After protein transfer, the membranes were washed once in TBST buffer (50 mM Tris, 150 mM NaCl, 0.05% Tween 20, pH 7.6) and then incubated in blocking buffer (TBST buffer with 5% non-fat milk powder). The membranes were then incubated sequentially with primary and secondary antibody. Protein

bands were visualized using the Enhanced Chemiluminescence kit (Pierce), and quantified in NIH ImageJ. β-actin was included as loading controls.

HIV-1 infections and cell lysate preparations

U373-MAGI-CCR5 target cells ($5X10^4$ cells/flask; obtained from NIH AIDS Research and Reference Reagent Program, and contributed by Drs. Michael Emerman and Adam Geballe). U373-MAGI-CCR5 cells express CD4 and human chemokine receptor CCR5 on the cell surface, which allows infection by HIV-1 R5 strains. These cells were infected with HIV-1_{SX}, which is a chimeric R5-tropic virus encoding the majority of the HIV-1 JRFL envelope protein in an HIV-1NL4–3 backbone. Forty-eight hours post-infection, cells were washed with distilled PBS and then prepared for lysis using lysis reagent according to the manufacturer's protocol (Cat # E1531, Promega). Cell lysates were harvested from HIV-infected or non-infected cells and used for Western blot analysis. HIV-1_{SX} was purchased from the Virology Core Facility, Center for AIDS Research at Baylor College of Medicine, Houston, TX.

Statistical analysis

Statistical analysis was performed with GraphPad Prism 5. Information of specific statistical tests and animal numbers is provided in figure legends. Data were expressed as means ± standard error of the mean (SEM).

RESULTS

Comparison of the HIV-1 viral loads and protein levels in the SDH of ‘pain-positive’ and ‘pain-negative’ HIV-1/AIDS patients

To identify the causative factor of HIV-associated pain, we first examined the potential contribution of HIV-1 viral load. We compared the copy numbers of the HIV-1 gag/pol RNA in the brain, cerebrospinal fluid (CSF) and blood plasma between the ‘pain-positive’ and ‘pain-negative’ HIV-1 infected patients. HIV-1 viral loads, as assessed by gag/pol RNA copy numbers, varied greatly in both patient groups. Nonetheless, we did not observe an obvious segregation of viral loads between the two groups (Fig. 1A). To directly measure the correlation between the viral loads and the pain status, we performed linear regression analysis. The correlation was not significant when viral loads from brain, CSF and plasma were either analyzed as a pool ($r=0.209$, $p=0.538$) or separately (brain viral load, $r=0.047$, $p=0.97$; CSF viral load, $r=0.438$, $p=0.562$; plasma viral load, $r=0.34$, $p=0.66$). We also performed immunoblotting analysis on HIV-1 p24, a molecular marker commonly used to gauge HIV-1 viral proliferation. The results showed that p24 did not significantly differ between the ‘pain-positive’ and ‘pain-negative’ HIV-1 patient groups (Fig. 1B, 1C). Thus, we did not observe increased HIV-1 replication or viral load in the ‘pain-positive’ HIV-1 patients.

Next, we tested whether the pain pathology was relevant to specific HIV-1 toxins. To this end, we compared the levels of neurotoxic HIV-1 proteins in the SDH of the ‘pain-positive’ and ‘pain-negative’ HIV-1 groups. HIV-1 envelope glycoprotein gp120 mediates the interaction between HIV-1 viral particles and target cells [26] and is one of the best

characterized HIV-1 neurotoxic proteins. Therefore, we first determined the levels of gp120 in the SDH by Western blot analysis. The results showed that gp120 protein in the SDH of 'pain-positive' HIV-1 patients was ~10 fold higher than in 'pain-negative' HIV-1 patients (Fig. 2A, B). This gp120 difference was significant in student's t-test ($p<0.05$; Fig. 2B). Because gp120 levels were drastically different in different patients, we also performed non-parametric comparison (Wilcoxon-Mann-Whitney test), which is less sensitive to the contribution of outliers. The gp120 difference between the 'pain-positive' and 'pain-negative' HIV-1 patients was significant in this test as well ($p<0.05$). In contrast, Tat, the HIV trans-activator of transcription that is implicated in HIV-1 associated neurotoxicity [27, 28], was markedly lower in the SDH of 'pain-positive' HIV-1 patients compared to 'pain-negative' HIV-1 patients (Fig. 2A, B). The specificity of the anti-gp120 and anti-Tat antibodies was confirmed using lysates from cells with or without HIV-1 infection (Fig. 2C). To estimate gp120 concentration in tissues, we performed semi-quantitative western blotting, including a series of purified gp120 on the same gel for generating a standard curve. Based on this analysis, we estimated that the levels of gp120 proteins in SDH were 0.13 and 1.29 pg per μg of total protein in 'pain negative' and 'pain-positive' HIV-1 patients, respectively. We also measured the level of another HIV-1 neurotoxic protein Vpr, and observed that Vpr did not significantly differ between the two groups (Fig. 2A, B). These results revealed that the development of the HIV-related pain is specifically associated with a higher level of gp120 protein in the SDH.

Characterization of pain behaviors in rodents after intrathecal injection of gp120

Based on the finding of higher gp120 levels in the SDH of 'pain-positive' HIV-1 patients (Fig. 2), we reasoned that introducing gp120 into the SDH in mice might create a relevant animal model. We used the approach of intrathecal injection (i.t.) to administer gp120, and then characterized pain behavior development in the mice. To test the development of mechanical allodynia, which is commonly manifested in HIV-1-infected patients, after i.t. gp120 administration mice were stimulated with von Frey filaments on the hind paws to measure paw withdrawal thresholds (PWT). Animals injected with equal amount of heat-inactivated gp120 were used as controls. Based on observations from preliminary studies using different protein amounts and the measurement of gp120 concentration in the SDH of HIV-1 patients described above, we chose a gp120 dose of 100ng/i.t. injection, which was estimated to give rise to a gp120 concentration of 10 pg/μg spinal protein, with the assumption of a final even diffusion of the protein throughout the spinal cord. Both $gp120_{Bal}$ (from $HIV\text{-}1_{R5}$ envelope) and $gp120_{IIIB}$ (from $HIV\text{-}1_{X4}$ envelope) were tested, and they showed similar potency in inducing mechanical allodynia (Fig. 3). The allodynia induced by a single injection lasted for at least 3 days before the PWT gradually returned to baseline (data not shown). As shown in Fig. 3, three injections of gp120 on days 0, 3 and 6 induced long-lasting allodynia that was clearly detectable at day 21. These data suggest that mice injected with either $gp120_{Bal}$ or $gp120_{IIIB}$ developed mechanical allodynia. For subsequent experiments, we used $gp120_{Bal}$, unless indicated otherwise.

Because visceral pain is common in HIV-1 patients [2, 29], we further tested if i.t. gp120 caused visceral hyperalgesia. Adult rats were used in this study. Visceral hyperalgesia was measured by electromyography (EMG) of visceromotor response (VMR) induced by

colorectal distension [25, 30]. We observed that, in comparison to control animals receiving vehicle (baseline) or heat-inactivated gp120, colorectal distension induced drastically higher EMG activity in experimental animals with gp120 injection (24 hr post injection), suggesting the development of robust visceral hyperalgesia in these animals (Fig. 4A). A detectable but non-significant increase in EMG was observed in animals that were injected with heat-inactivated gp120 (Fig. 4A). Intriguingly, the gp120-induced visceral hyperalgesia was very long-lasting. Even though a progressive decrease occurred, a clear manifestation of the visceral hyperalgesia continued at least 2 weeks after a single gp120 injection (Fig. 4B).

Peripheral neuropathy in the i.t. gp120 mouse model

Peripheral neuropathy is a hallmark of the neurological pathology that is commonly observed with the manifestation of HIV-associated chronic pain [22, 31, 32]. Thus, it was relevant to determine whether the i.t. gp120 mouse model developed peripheral neuropathy. Preliminary studies with single i.t. gp120 injection indicated the development of neuropathy in the plantar skin of the hind paw. To robustly induce neuropathy, we injected gp120 three times with two-day intervals. The animals were sacrificed on day 7, 14 or 21 after the first injection, and the plantar skin of the hind paw was collected for PGP9.5 immunostaining. Similar to naïve animals, animals with injections of heat-inactivated gp120 showed abundant PGP9.5-stained nerve fibers in the epidermis and fiber bundles in the dermis; these fibers were intact (Fig. 5A1). Mice injected with gp120 displayed progressive degeneration of the PGP9.5-labelled nerves. Fragmented nerves were first observed on day 7 (Fig. 5A2). On day 14, many nerve fibers in the epidermis had undergone morphological fragmentation (Fig. 5A3). On day 21 intact PGP9.5-labelled intraepidermal nerve fibers (IENF) were sparse (Fig. 5A4). Similar to previous reports [33, 34], the density of IENF in the hind paw plantar skin from control mice that received i.t. boiled gp120 on day 21 was 35 ± 2.74. Repeated i.t. injections of gp120 resulted in a progressive decrease of IENF in the epidermis (Fig. 5B); the IENF at 1, 2, or 3 weeks were 31.25 ± 3.82, 11.0 ± 2.92 or 8.75 ± 1.12, respectively.

The i.t. gp120 injections also caused degeneration of the nerve fibers innervating eccrine glands in the dermis of the hind paw. In control animals, the PGP9.5-labbled nerve fibers in eccrine glands were neatly organized around the gland cells (Fig. 5C1, C2). On day 7, a combination of normal, swollen and atrophied axons were found in the eccrine glands (Fig. 5C3, C4). On day 14, only swollen and atrophied axons were visible in the glands (Fig. 5C5, C6). On day 21, fibers labeled by PGP9.5 largely disappeared, leaving only sparse fragments with faint labeling (Fig. 5C7, C8).

These findings illustrate that the i.t. gp120 treatment in mice produced distal sensory and sudomotor nerve fiber damage, and indicate that gp120 induces neuropathy in different peripheral innervations. The nerve atrophy may model the peripheral neuropathy developed in HIV-1 infected patients [35-37].

Comparison of the glial activation profiles in the SDH of 'pain-positive' HIV-1 patients and the i.t. gp120 model

We recently reported astroglial reactivation in the SDH of 'pain-positive' HIV-1 patients[22]. Hence, we carried out comparative analyses to test if there were similarities in the expression profiles of glial markers in the SDH of the 'pain-positive' HIV-1 patients and the i.t. gp120 model. As shown in Fig. 3, we used the model of repeated i.t. gp120 injection and performed analyses on the SDH at day 7, 14 or 21. Similar to the SDH of the 'pain-positive' HIV-1 patients, the SDH of the i.t. gp120 model at all of time points showed significant up-regulation of glial fibrillary acidic protein (GFAP), an astrocytic marker (Fig. 6A, B). As we reported previously[22], microglial markers such as Iba1 were not significantly up-regulated in the 'pain-positive' HIV-1 patients (Fig. 6A, C). However, compared with control animals that were i.t.-injected with heat-inactivated gp120, the microglial/macrophage marker Iba1 was markedly increased at all of the examined time points in the SDH of the i.t. gp120 model (Fig. 6A, C).

Glial activation is often coupled to the up-regulation of pro-inflammatory cytokines [38]. Indeed, both TNF-α and IL-1β were up-regulated in the SDH of the 'pain-positive' HIV-1 patients (Fig. 6A, D, E). TNFα and IL-1β were also up-regulated in the SDH of the i.t. gp120 model (Fig. 6A, D, E).

Synapse loss in the SDH of the 'pain-positive' HIV-1 patients and the gp120 model

Next, we investigated whether synapses in the SDH were affected in the 'pain-positive' HIV-1 patients and the i.t. gp120 mouse model (with repeated i.t. injections as in Fig. 3). Immunoblot analysis showed that the level of PSD-95, a post-synaptic marker, was decreased by 48% in the SDH of 'pain-positive' HIV-1 patients, compared with non-HIV patients (Fig. 7A, B). By contrast, the PSD-95 level in the SDH of 'pain-negative' HIV-1 patients was not significantly different from non-HIV controls (Fig. 7A, B). In the i.t. gp120 model, the PSD-95 levels did not decrease at days 7 and 14 (Fig. 7A, B). However, the level dropped to 47% of the control at day 21 (Fig. 7A, B). These data suggest the degeneration of post-synaptic structures in both the 'pain-positive' HIV-1 patients and the i.t. gp120 model at day 21. The pre-synaptic component was also analyzed, using the pre-synaptic marker, synapsin I. Similar to PSD-95, we observed a specific decrease of synapsin I in the SDH of 'pain-positive' HIV-1 patients compared with non-HIV controls (Fig. 7A, C). Again, in the i.t. gp120 model, synapsin I decreased only at day 21 but not at days 7 and 14 (Fig. 7A, C), indicating pre-synaptic degeneration. To assess the potential abnormalities of the synaptic transmission in the HIV-1 patients and the i.t. gp120 model, we determined the protein level of subunit 1 of the NMDA receptor (NR1), a major glutamate receptor that is critical for synaptic plasticity. Consistent with the findings for PSD-95 and synapsin I, we found that NR1 is markedly (78%) decreased in the 'pain-positive' HIV-1 patients, compared with non-HIV controls (Fig. 7A, D). NR1 decrease was not observed in 'pain-negative' HIV-1 patients (Fig. 7A, D). In the i.t. gp120 model, the protein level of NR1 also decreased on day 21 but not on days 7 and 14 (Fig. 7A, D). Thus, there was a striking similarity between the down-regulation of synaptic markers in the SDH of the 'pain-positive' HIV-1 patients and the i.t. gp120 model at day 21.

Dysregulation of central sensitization-related signaling pathways in the 'pain-positive' HIV-1 patients and the gp120 model

Previous studies on animal models revealed critical signal transduction pathways in the SDH for the development of central sensitization, a maladaptive neural plasticity implicated in the pathogenesis of chronic pain. One of these pathways is the MAPK signaling pathway [39-42]. Therefore, we sought to compare the activity of MAP kinases, including ERK and JNKs in the SDH of the 'pain-positive' HIV-1 patients and the i.t. gp20 model. We found that phosphorylated JNK (p-JNK, Thr183/Tyr185; active JNK) was increased 1.6 fold in the SDH of 'pain-positive' but not the 'pain-negative' HIV-1 patients, compared to non-HIV control patients (Fig. 8A, B). Recent work indicated that JNKs are activated in reactive astrocytes in the SDH of chronic pain models [43]. The increase of p-JNKs is consistent with the activation of astrocytes in the SDH of the 'pain-positive' HIV-1 patients (Fig. 6A, B). We also observed a p-JNK increase in the i.t. gp120 mice, from days 7 to 21 (Fig. 8A, B). Similar to the profiles of JNK activation, p-ERK (Thr202/Tyr204) specifically increased in the SDH of 'pain-positive' HIV-1 patients (~7 fold compared to non-HIV control patients) (Fig. 8A, C), as well as in the i.t. gp120 mice (compared to i.t. heat-inactivated controls, Fig. 8A, C). In addition to MAPK signaling, CaMKII signaling also plays an important role in central sensitization signaling [44, 45]. We found that p-αCaMKII (p-T286) was increased in the 'pain-positive' HIV patients but not in 'pain-negative' HIV patients (compared to non-HIV control patients) and the i.t. gp120 model (compared to i.t. heat-inactivated gp120 controls) (Fig. 8A, D). Taken together, these data suggest that the changes in signaling pathways critical for central sensitization found in pain-positive HIV-1 patients are mirrored in the i.t. gp120 mouse model.

DISCUSSION

The pathogenic mechanisms of HIV-associated pain remain to be elucidated. To understand these mechanisms, it is critical to identify the HIV-relevant factor(s) that cause chronic pain. The present study reveals that in the SDH, the first CNS pain processing center, HIV-1 gp120 is approximately 10-fold higher in the HIV-1 patients with chronic pain, compared to the 'pain-negative' HIV-1 patients. Importantly, this pain-associated difference in the gp120 level does not appear to be associated with an increase of viral load in plasma or CSF. This finding suggests that the higher gp120 levels do not require an enhancement of systemic and/or CNS viral replication. Instead, it suggests that the synthesis of pathogenic gp120 is independent of viral assembly. Consistent with this interpretation, the levels of other HIV-1 proteins, including Tat, Vpr and P24, were not associated with the chronic pain status. The relatively low expression of Tat in the SDH of 'pain-positive' HIV-1 patients is particularly interesting because this HIV-1 protein is a transactivator of transcription that functions in the early stages of the HIV-1 life cycle. Its apparently low level in the 'pain-positive' HIV-1 patients provides a mechanistically relevant indicator that further supports the concept that the development of HIV-associated chronic pain and the up-regulation of gp120 are not caused by increased HIV-1. Taken together, our results suggest that gp120 is a potential viral agent that may critically contribute to the pathogenesis of HIV-associated chronic pain in human patients.

The gp120 is a late structural protein in viral replication. It is unclear how the level of this late protein can be selectively increased in the SDH of 'pain-positive' HIV-1 patients when Tat is low. One may envision potential mechanisms of increased stability or synthesis of this protein. Considering the possibility of increased synthesis of gp120, it is interesting to note that the *env* gene is located near the downstream end of the HIV-1 pro-viral genome. Because of the essential role of Tat in HIV-1 transcription, when Tat is at a low level, one would expect that the elongation of many viral transcripts may stop prematurely and thus may not contain the *env* RNA. The counter-intuitive findings of the combination of high gp120 and low Tat protein levels suggest a potential intriguing mechanism(s) that selectively stimulates gp120 synthesis from full-length viral transcripts. Although the cause responsible for the lower level of Tat in the 'pain-positive' HIV-1 patients is unclear, in theory, it could result from either an increase of protein degradation or a reduction of protein synthesis. Interestingly, in 'pain-negative' HIV patients, Tat was relatively high while gp120 was low (Fig. 2A, 2B). Among other possibilities, it would be intriguing to know if this was a result of HIV-protease inhibitors, which act downstream of Tat and suppress gp160 (the gp120 precursor protein) processing.

The finding of higher levels of gp120 in the SDH of HIV-1 patients with chronic pain suggests that gp120 is a candidate of causative HIV-1 agents. This idea is supported by further studies on the mouse model with i.t. injection of gp120 to mimic the increased gp120 in the SDH of human patients. We compared the behavioral, neurological, glial, synaptic and molecular phenotypes in the i.t. gp120 mouse model and the HIV-1 patients. The results revealed extensive similarities between the patients and the animal model. Consistent with previous reports [8, 10], the mouse model developed mechanical allodynia, which is a common pain symptom that develops in HIV-1 patients [29, 46]. Furthermore, similar to many HIV-1 patients who develop visceral pain [2, 29], the i.t. gp120 model also developed visceral hyperalgesia.

Peripheral neuropathy is common in HIV-1 patients who manifest chronic pain [6, 47]. We observed that i.t. gp120 induced progressive degeneration of nerve fibers in the plantar skin of hind paws. Thus, the i.t. gp120 mouse model recapitulates the phenotype of peripheral neuropathy in 'pain-positive' HIV-1 patients. Consistent with our results, previous studies showed that gp120 in transgenic mice or gp120 applied to sciatic nerves facilitated antiretroviral agent-induced neuropathy [7, 9, 12]. Our results suggest that i.t.-injected gp120 is sufficient to cause degeneration of peripheral axons. This finding implies that the gp120 from residual infected cells in the CNS may still cause peripheral nerve damage. One way by which gp120 may cause peripheral neuropathy is to directly stimulate sensory neurons (e.g. via their central termini). Gp120 can stimulate neurons via an HIV-1 co-receptor (e.g. CXCR4), which functionally couples to the NMDA receptor[48-52]. Neuron stimulation by gp120 was shown to cause Ca^{2+} overloading-mediated neurotoxicity which ultimately leads to axonal damage of sensory neurons[17, 53]. Both Ca^{2+} influx and Ca^{2+} release from intracellular stores elicited by gp120 could contribute to the neurotoxicity[17, 52]. In addition, gp120 may also elicit detrimental factors from nearby cells to cause neurotoxicity. For instance, studies from Weswani *et al.* reveal that gp120 stimulates CXCR4 on Schwann cells

to elicit the release of RANTES, which in turn induces neurotoxic autocrine secretion of TNF-α from DRG neurons[54].

We previously described the astroglial activation and up-regulation of TNF-α and IL-1β in the SDH of 'pain-positive' (but not 'pain-negative') HIV-1 patients [22]. We confirmed these findings in this study (Fig. 6, $p>0.05$). Many studies have suggested important roles of astrocyte reactivation[43, 55-61], TNF-α[62] and IL-1β[63] in pathological pain. Similarly, GFAP up-regulation was observed in the i.t. gp120 model. Because of the proposed roles of activated astrocytes in the pathogenesis of chronic pain [43, 55-61], the i.t. gp120 model may provide an HIV-associated pain-relevant *in vivo* system to study the mechanism and pathogenic significance of astrocyte activation in the SDH. By contrast, although we did not detect microglial activation (as judged by the Iba1 level) in the SDH of 'pain-positive' HIV-1 patients [22], a marked increase of Iba1 protein was observed in the i.t. gp120 model, indicating the activation of microglia/macrophages. In considering this discrepancy, it is worth noting that the characterization of microglial activation in the i.t. gp120 model in this study was restricted within 3 weeks after 1st gp120 administration. The gp120-stimulated microglial activation may return to a resting state later, as suggested by previous studies [10]. Because the human postmortem tissues were likely taken from patients long after the initial HIV-1 infection, the microglia that reacted to initial HIV-1 infection may have returned to a resting state.

We also compared the profiles of synaptic markers in the SDH of HIV-1 patients and the gp120 model. Our data revealed a striking similarity between the 'pain-positive' HIV-1 patient and the i.t. gp120 model three weeks after gp120 administration. We observed a decrease of pre- and post-synaptic markers and NMDARs in the SDH of the i.t. gp120 model at day 21. These findings indicated that i.t. gp120 induced synaptic degeneration. Because the decrease of synaptic markers was not detected before day 14 in the model, the gp120-induced synaptic degeneration *in vivo* is a chronic process, although in primary neuron cultures gp120 can cause synapse loss in a shorter time frame [64]. Synapse loss was also observed in gp120 transgenic mice [65, 66]. In agreement with our findings, previous studies reported cortical synapse loss in the HIV-1 patients [67, 68].

Central sensitization is thought to be a spinal cellular basis of chronic pain [69]. Indeed, we observed that several signaling pathways, including JNK [56, 70], ERK [71, 72] and CaMKII [44, 45] signaling, which are important for the expression of central sensitization in animal models, were activated in the SDH of the 'pain-positive' (but not in the 'pain-negative') HIV-1 patients. These data provide support for the involvement of central sensitization in the pathogenesis of human chronic pain. Similarly, we also observed activation of these signaling pathways in the i.t. gp120 model.

In summary, our analysis on the postmortem specimens of HIV-1/AIDS patients revealed, for the first time, the pain-associated increase of gp120 in the SDH. In addition, our systematic comparative analyses reveal remarkable similarities between the 'pain-positive' HIV-1 patients and the i.t. gp120 mice. The results provide evidence for gp120 as a potential pathogenically relevant factor of HIV-associated neuropathic pain.

Acknowledgments

We thank the NIH AIDS Research and Reference Reagent Program for providing the gp120 protein, antibodies against HIV-1 proteins and U373-MAGI-CCR5 cells. We thank Edward Siwak, Ph.D., Associate Director of Virology Core Facility, Center for AIDS Research at Baylor College of Medicine, Houston, TX, for providing HIV-1_{SX}. This work was supported by the following grants: R01-NS079166 and R01-DA036165 (SJT), U24MH100930, U01MH083507, R24NS45491, and R24 MH59656 (BBG), 5R01DK088796 (SKS), HL088999 (MRF), RO1NS027910 and RO1DA027460 (SMC).

REFERENCES

1. Gendelman, HE.; Grant, I.; Everall, IP., et al. The Neurobiology of AIDS. 3rd ed.. Oxford University Press; Oxford: 2012.
2. Hewitt DJ, McDonald M, Portenoy RK, et al. Pain syndromes and etiologies in ambulatory AIDS patients. Pain. 1997; 70:117. [PubMed: 9150284]
3. Mirsattari SM, Power C, Nath A. Primary Headaches in HIV-Infected Patients. Headache: The Journal of Head and Face Pain. 1999; 39:3.
4. Evers S, Wibbeke B, Reichelt D, et al. The impact of HIV infection on primary headache. Unexpected findings from retrospective, cross-sectional, and prospective analyses. Pain. 2000; 85:191. [PubMed: 10692618]
5. Aouizerat BE, Miaskowski CA, Gay C, et al. Risk Factors and Symptoms Associated With Pain in HIV-Infected Adults. Journal of the Association of Nurses in AIDS care. 2010; 21:125–133. [PubMed: 20116299]
6. Griffin JW, Crawford TO, Tyor WR, et al. Predominantly sensory neuropathy in AIDS: distal axonal degeneration and unmyelinated fiber loss. Neurology. 1991; 41:374.
7. Wallace VCJ, Blackbeard J, Segerdahl AR, et al. Characterization of rodent models of HIV-gp120 and anti-retroviral-associated neuropathic pain. Brain. 2007; 130:2688–2702. [PubMed: 17761732]
8. Milligan ED, Mehmert KK, Hinde JL, et al. Thermal hyperalgesia and mechanical allodynia produced by intrathecal administration of the human immunodeficiency virus-1 (HIV-1) envelope glycoprotein, gp120. Brain Research. 2000; 861:105. [PubMed: 10751570]
9. Herzberg U, Sagen J. Peripheral nerve exposure to HIV viral envelope protein gp120 induces neuropathic pain and spinal gliosis. Journal of Neuroimmunology. 2001; 116:29. [PubMed: 11311327]
10. Milligan ED, O'Connor KA, Nguyen KT, et al. Intrathecal HIV-1 Envelope Glycoprotein gp120 Induces Enhanced Pain States Mediated by Spinal Cord Proinflammatory Cytokines. The Journal of Neuroscience. 2001; 21:2808–2819. [PubMed: 11306633]
11. Oh SB, Tran PB, Gillard SE, et al. Chemokines and Glycoprotein120 Produce Pain Hypersensitivity by Directly Exciting Primary Nociceptive Neurons. The Journal of Neuroscience. 2001; 21:5027–5035. [PubMed: 11438578]
12. Keswani SC, Jack C, Zhou C, Hoke A. Establishment of a Rodent Model of HIV-Associated Sensory Neuropathy. The Journal of Neuroscience. 2006; 26:10299–10304. [PubMed: 17021185]
13. Wallace VCJ, Blackbeard J, Pheby T, et al. Pharmacological, behavioural and mechanistic analysis of HIV-1 gp120 induced painful neuropathy. Pain. 2007; 133:47. [PubMed: 17433546]
14. Zheng W, Ouyang H, Zheng X, et al. Glial TNFalpha in the spinal cord regulates neuropathic pain induced by HIV gp120 application in rats. Molecular Pain. 2011; 7:40. [PubMed: 21599974]
15. Acharjee S, Noorbakhsh F, Stemkowski PL, et al. HIV-1 viral protein R causes peripheral nervous system injury associated with in vivo neuropathic pain. The FASEB Journal. 2010; 24:4343–4353.
16. Bhangoo S, Ripsch M, Buchanan D, et al. Increased chemokine signaling in a model of HIV1-associated peripheral neuropathy. Molecular Pain. 2009; 5:48. [PubMed: 19674450]
17. Höke A, Morris M, Haughey NJ. GPI-1046 protects dorsal root ganglia from gp120-induced axonal injury by modulating store-operated calcium entry. Journal of the Peripheral Nervous System. 2009; 14:27. [PubMed: 19335537]

18. Melli G, Keswani SC, Fischer A, et al. Spatially distinct and functionally independent mechanisms of axonal degeneration in a model of HIV-associated sensory neuropathy. Brain. 2006; 129:1330–1338. [PubMed: 16537566]
19. Keswani SC, Leitz GJ, Hoke A. Erythropoietin is neuroprotective in models of HIV sensory neuropathy. Neuroscience Letters. 2004; 371:102. [PubMed: 15519737]
20. Chi X, Amet T, Byrd D, et al. Direct Effects of HIV-1 Tat on Excitability and Survival of Primary Dorsal Root Ganglion Neurons: Possible Contribution to HIV-1-Associated Pain. PLoS ONE. 2011; 6:e24412. [PubMed: 21912693]
21. Morgello S, Gelman BB, Kozlowski PB, et al. The National NeuroAIDS Tissue Consortium:a new paradigm in brain banking with an emphasis on infectious disease. Neuropathology and Applied Neurobiology. 2001; 27:326–335. [PubMed: 11532163]
22. Shi Y, Gelman BB, Lisinicchia JG, Tang S-J. Chronic-pain-associated astrocytic reaction in the spinal cord dorsal horn of HIV-infected patients. J Neurosci. 2012; 32:10833–10840. [PubMed: 22875918]
23. Hylden JLK, Wilcox GL. Intrathecal morphine in mice: A new technique. European Journal of Pharmacology. 1980; 67:313. [PubMed: 6893963]
24. Callahan BL, Gil AS, Levesque A, Mogil JS. Modulation of mechanical and thermal nociceptive sensitivity in the laboratory mouse by behavioral state. J Pain. 2008:9.
25. Winston JH, Xu G, Sarna SK. Adrenergic Stimulation Mediates Visceral Hypersensitivity to Colorectal Distension Following Heterotypic Chronic Stress. Gastroenterology. 2010; 138:294–304. [PubMed: 19800336]
26. Kwong PD, Wyatt R, Robinson J, et al. Structure of an HIV gp120 envelope glycoprotein in complex with the CD4 receptor and a neutralizing human antibody. Nature. 1998; 393:648. [PubMed: 9641677]
27. Romani B, Engelbrecht S, Glashoff RH. Functions of Tat: the versatile protein of human immunodeficiency virus type 1. J Gen Virol. 2010; 91:1–12. [PubMed: 19812265]
28. Magnuson DS, Knudsen BE, Geiger JD, et al. Human immunodeficiency virus type 1 tat activates non-N-methyl-D-aspartate excitatory amino acid receptors and causes neurotoxicity. Ann Neurol. 1995; 37:373–380. [PubMed: 7695237]
29. Newshan G. Pain in human immunodeficiency virus disease. Semin Oncol Nurs. 1997; 13:36–41. [PubMed: 9048435]
30. Winston JH, Sarna SK. Developmental Origins of Functional Dyspepsia-Like Gastric Hypersensitivity in Rats. Gastroenterology. 2013; 144:570–579. [PubMed: 23142231]
31. Evans SR, Ellis RJ, Chen H, et al. Peripheral neuropathy in HIV: prevalence and risk factors. AIDS. 2011; 25:919–928. [PubMed: 21330902]
32. Cao L, Butler MB, Tan L, et al. Murine Immunodeficiency Virus-Induced Peripheral Neuropathy and the Associated Cytokine Responses. The Journal of Immunology. 2012; 189:3724–3733. [PubMed: 22956581]
33. Kellogg AP, Wiggin TD, Larkin DD, et al. Protective Effects of Cyclooxygenase-2 Gene Inactivation Against Peripheral Nerve Dysfunction and Intraepidermal Nerve Fiber Loss in Experimental Diabetes. Diabetes. 2007; 56:2997–3005. [PubMed: 17720896]
34. Ko M-H, Chen W-P, Hsieh S-T. Neuropathology of Skin Denervation in Acrylamide-Induced Neuropathy. Neurobiology of Disease. 2002; 11:155. [PubMed: 12460555]
35. Compostella C, Compostella L, D'Elia R. The symptoms of autonomic dysfunction in HIV-positive Africans. Clin Auton Res. 2008; 18:6–12. [PubMed: 18080822]
36. Boger MS, Hulgan T, Haas DW, et al. Measures of small-fiber neuropathy in HIV infection. Autonomic Neuroscience. 2012; 169:56–61. [PubMed: 22542355]
37. Kamerman PR, Moss PJ, Weber J, et al. Pathogenesis of HIV-associated sensory neuropathy: evidence from in vivo and in vitro experimental models. Journal of the Peripheral Nervous System. 2012; 17:19–31. [PubMed: 22462664]
38. Watkins LR, Deak T, Silbert L, et al. Evidence for involvement of spinal cord glia in diverse models of hyperalgesia. Proc. Soc. Neurosci. 1995; 21:879.
39. Ji R-R, Baba H, Brenner GJ, Woolf CJ. Nociceptive-specific activation of ERK in spinal neurons contributes to pain hypersensitivity. Nat Neurosci. 1999; 2:1114. [PubMed: 10570489]

40. Jin S-X, Zhuang Z-Y, Woolf CJ, Ji R-R. p38 Mitogen-Activated Protein Kinase Is Activated after a Spinal Nerve Ligation in Spinal Cord Microglia and Dorsal Root Ganglion Neurons and Contributes to the Generation of Neuropathic Pain. The Journal of Neuroscience. 2003; 23:4017–4022. [PubMed: 12764087]
41. Gao YJ, Ji RR. c-Fos and pERK, which is a better marker for neuronal activation and central sensitization after noxious stimulation and tissue injury? Open Pain J. 2009; 2:11–17. [PubMed: 19898681]
42. Gao Y-J, Cheng J-K, Zeng Q, et al. Selective inhibition of JNK with a peptide inhibitor attenuates pain hypersensitivity and tumor growth in a mouse skin cancer pain model. Experimental Neurology. 2009; 219:146. [PubMed: 19445931]
43. Gao Y-J, Xu Z-Z, Liu Y-C, et al. The c-Jun N-terminal kinase 1 (JNK1) in spinal astrocytes is required for the maintenance of bilateral mechanical allodynia under a persistent inflammatory pain condition. Pain. 2010; 148:309. [PubMed: 20022176]
44. Fang L, Wu J, Lin Q, Willis WD. Calcium-Calmodulin-Dependent Protein Kinase II Contributes to Spinal Cord Central Sensitization. The Journal of Neuroscience. 2002; 22:4196–4204. [PubMed: 12019337]
45. Crown ED, Gwak YS, Ye Z, et al. Calcium/calmodulin dependent kinase II contributes to persistent central neuropathic pain following spinal cord injury. Pain. 2012; 153:710–721. [PubMed: 22296735]
46. Bouhassira D, Attal N, Willer J-C, Brasseur L. Painful and painless peripheral sensory neuropathies due to HIV infection: a comparison using quantitative sensory evaluation. Pain. 1999; 80:265–272. [PubMed: 10204739]
47. Elliott, KJ.; McArthur, JC.; Simpson, DM. Peripheral Neuropathy.. In: Gendelman, HE.; Grant, I.; Everall, IP., et al., editors. The Neurology of AIDS. 3rd ed.. Oxford University Press; Oxford: 2012. p. 536-545.
48. Pandey V, Bolsover SR. Immediate and Neurotoxic Effects of HIV Protein gp120 Act through CXCR4 Receptor. Biochemical and Biophysical Research Communications. 2000; 274:212. [PubMed: 10903920]
49. Kaul M, Lipton SA. Chemokines and activated macrophages in HIV gp120-induced neuronal apoptosis. Proceedings of the National Academy of Sciences. 1999; 96:8212–8216.
50. Nath A, Haughey NJ, Jones M, et al. Synergistic neurotoxicity by human immunodeficiency virus proteins Tat and gp120: protection by memantine. Ann Neurol. 2000; 47:186–194. [PubMed: 10665489]
51. Lipton SA, Sucher NJ, Kaiser PK, Dreyer EB. Synergistic effects of HIV coat protein and NMDA receptor-mediated neurotoxicity. Neuron. 1991; 7:111. [PubMed: 1676893]
52. Lannuzel A, Lledo PM, Lamghitnia HO, et al. HIV-1 envelope proteins gp120 and gp160 potentiate NMDA-induced [Ca2+]i increase, alter [Ca2+]i homeostasis and induce neurotoxicity in human embryonic neurons. Eur J Neuroeci. 1995; 7:2285–2293.
53. Dreyer E, Kaiser P, Offermann J, Lipton S. HIV-1 coat protein neurotoxicity prevented by calcium channel antagonists. Science. 1990; 248:364–367. [PubMed: 2326646]
54. Keswani SC, Polley M, Pardo CA, et al. Schwann cell chemokine receptors mediate HIV-1 gp120 toxicity to sensory neurons. Annals of Neurology. 2003; 54:287. [PubMed: 12953261]
55. Garrison CJ, Dougherty PM, Kajander KC, Carlton SM. Staining of glial fibrillary acidic protein (GFAP) in lumbar spinal cord increases following a sciatic nerve constriction injury. Brain Research. 1991; 565:1–7. [PubMed: 1723019]
56. Gao Y-J, Zhang L, Samad OA, et al. JNK-Induced MCP-1 Production in Spinal Cord Astrocytes Contributes to Central Sensitization and Neuropathic Pain. The Journal of Neuroscience. 2009; 29:4096–4108. [PubMed: 19339605]
57. Gao Y-J, Zhang L, Ji R-R. Spinal injection of TNF-α-activated astrocytes produces persistent pain symptom mechanical allodynia by releasing monocyte chemoattractant protein-1. Glia. 2010; 58:1871. [PubMed: 20737477]
58. Gwak YS, Hulsebosch CE. Remote astrocytic and microglial activation modulates neuronal hyperexcitability and below-level neuropathic pain after spinal injury in rat. Neuroscience. 2009; 161:895–903. [PubMed: 19332108]

59. Hulsebosch CE. Gliopathy ensures persistent inflammation and chronic pain after spinal cord injury. Experimental Neurology. 2008; 214:6–9. [PubMed: 18708053]
60. Zhuang Z-Y, Wen Y-R, Zhang D-R, et al. A Peptide c-Jun N-Terminal Kinase (JNK) Inhibitor Blocks Mechanical Allodynia after Spinal Nerve Ligation: Respective Roles of JNK Activation in Primary Sensory Neurons and Spinal Astrocytes for Neuropathic Pain Development and Maintenance. The Journal of Neuroscience. 2006; 26:3551–3560. [PubMed: 16571763]
61. Zhang H, Yoon S-Y, Zhang H, Dougherty PM. Evidence That Spinal Astrocytes but Not Microglia Contribute to the Pathogenesis of Paclitaxel-Induced Painful Neuropathy. The Journal of Pain. 2012; 13:293–303. [PubMed: 22285612]
62. Leung L, Cahill C. TNF-alpha and neuropathic pain - a review. Journal of Neuroinflammation. 2010; 7:27. [PubMed: 20398373]
63. Ren K, Torres R. Role of interleukin-1$\hat{1}^2$ during pain and inflammation. Brain Research Reviews. 2009; 60:57. [PubMed: 19166877]
64. Kim HJ, Shin AH, Thayer SA. Activation of Cannabinoid Type 2 Receptors Inhibits HIV-1 Envelope Glycoprotein gp120-Induced Synapse Loss. Molecular Pharmacology. 2011; 80:357–366. [PubMed: 21670103]
65. Toggas SM, Masliah E, Rockenstein EM, et al. Central nervous system damage produced by expression of the HIV-1 coat protein gpl20 in transgenic mice. Nature. 1994; 367:188–193. [PubMed: 8114918]
66. Maung R, Medders K, Sejbuk N, et al. Genetic Knockouts Suggest a Critical Role for HIV Co-Receptors in Models of HIV gp120-Induced Brain Injury. Journal of Neuroimmune Pharmacology. 2012; 7:306–318. [PubMed: 22124968]
67. Wiley CA, Masliah E, Morey M, et al. Neocortical damage during HIV infection. Ann Neurol. 1991; 29:651–657. [PubMed: 1909852]
68. Everall IP, Heaton RK, Marcotte TD, et al. Cortical synaptic density is reduced in mild to moderate human immunodeficiency virus neurocognitive disorder. Brain Pathol. 1999; 9:209–217. [PubMed: 10219738]
69. Latremoliere A, Woolf CJ. Central Sensitization: A Generator of Pain Hypersensitivity by Central Neural Plasticity. The Journal of Pain. 2009; 10:895–926. [PubMed: 19712899]
70. Gao Y-J, Ji R-R. Activation of JNK pathway in persistent pain. Neuroscience Letters. 2008; 437:180. [PubMed: 18455869]
71. Gao Y-J, Ji R-R. Light touch induces ERK activation in superficial dorsal horn neurons after inflammation: involvement of spinal astrocytes and JNK signaling in touch-evoked central sensitization and mechanical allodynia. Journal of Neurochemistry. 2010; 115:505. [PubMed: 20722971]
72. Ji R-R, Gereau RW Iv, Malcangio M, Strichartz GR. MAP kinase and pain. Brain Research Reviews. 2009; 60:135. [PubMed: 19150373]

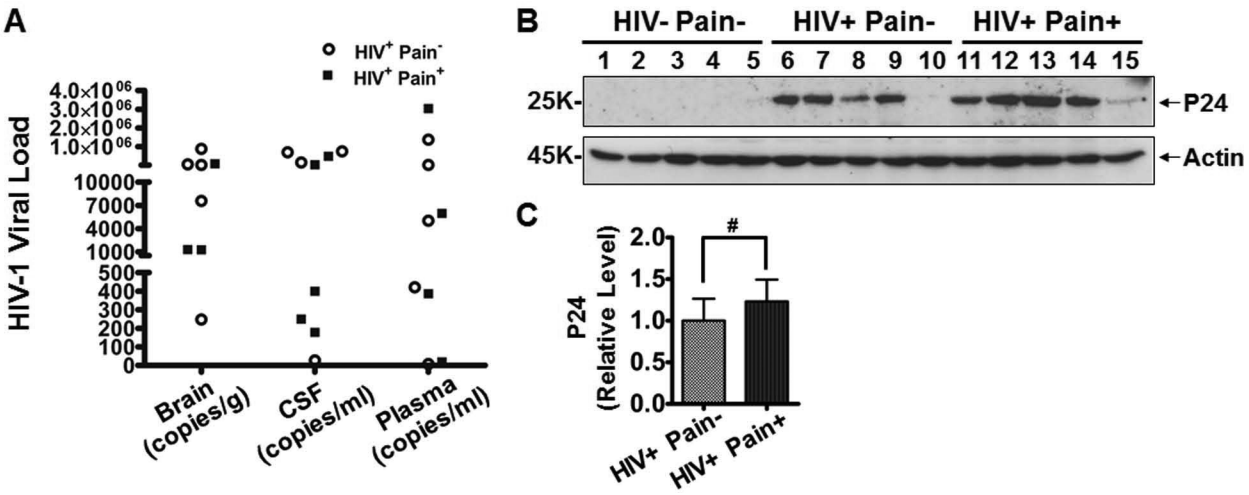

Figure 1.

Comparison of HIV-1 viral loads in the 'pain-positive' and 'pain-negative' HIV-infected patients. A. HIV-1 viral loads as measured by the copy number of gag/pol RNA. Shown are the copy numbers of individual patients. B. Immunoblotting of P24 protein in the SDH in 'pain-positive' and 'pain-negative' HIV-infected patients. C. Quantitative summary of B. Error bars: SEM (#, $p>0.05$, n=5/group, student's t test).

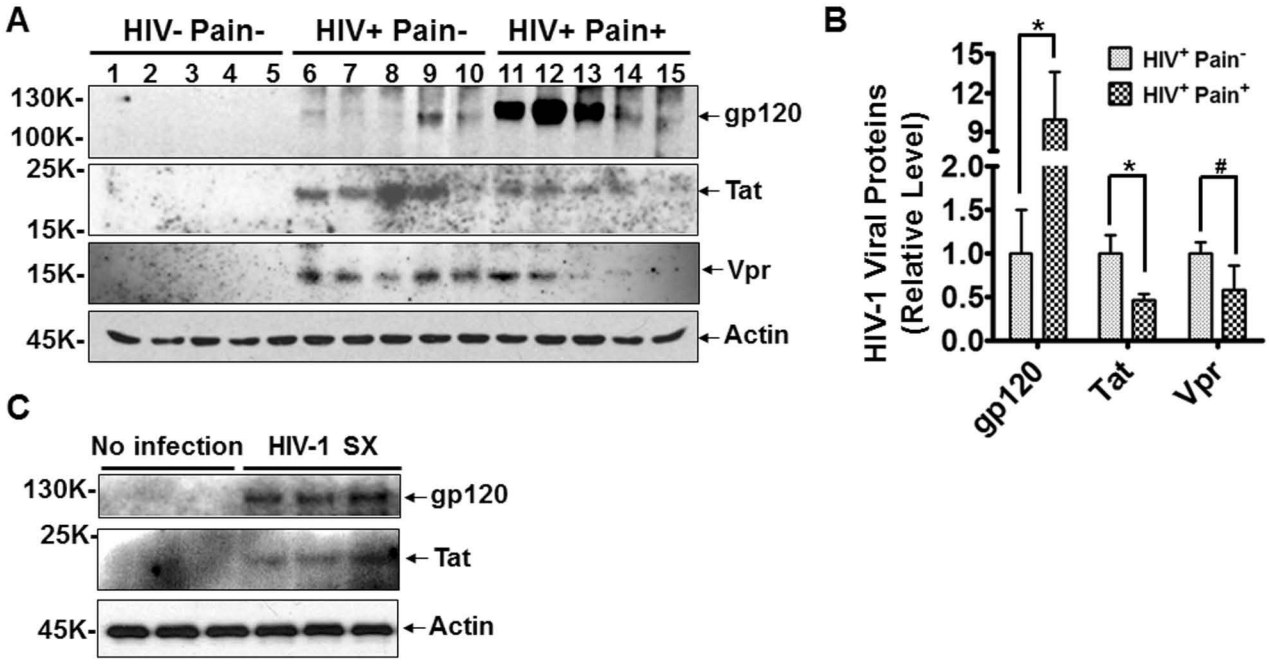

Figure 2.

Comparison of the levels of toxic HIV-1 protein in the 'pain-positive' and 'pain-negative' HIV-infected patients. A. Immunoblots of gp120, Tat and Vpr in the SDH of postmortem tissues. Gp120 protein (but not Tat or Vpr) specifically increased in the SDH of 'pain-positive' HIV patients. No specific bands of these proteins were detected in the non-HIV patients. B. Quantitative summary of gp120, Tat, Vpr and Tat. C. Immunoblots of lysates of cultured cells with or without HIV-1_{SX} infection. Error bars: SEM (*, $p<0.05$; #, $p>0.05$; n=5/group, student's t test).

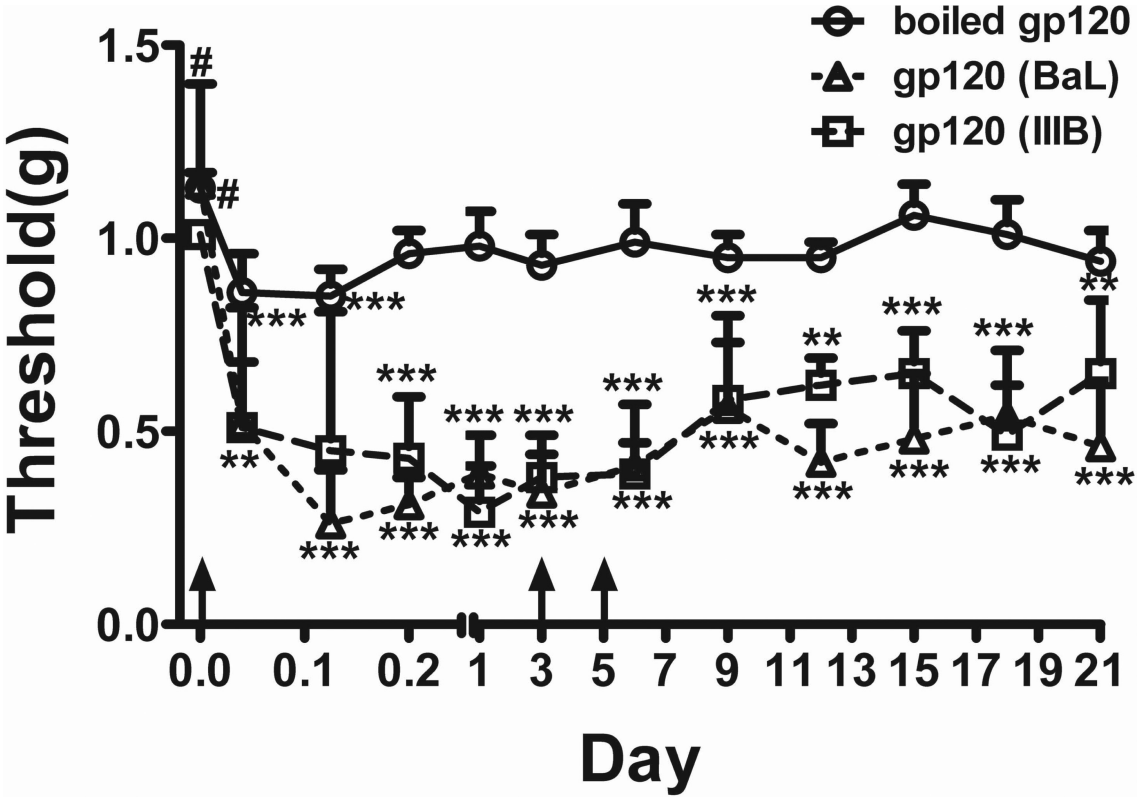

Figure 3.

Intrathecal injection (i.t.) of gp120 caused mechanical allodynia in mice. Threshold of mechanical pain in the hind paw was measured by von Frey testing. Numbers of animals used in each group: boiled $gp120_{IIIB}$, 11 mice; $gp120_{Bal}$: 6 mice; $gp120_{IIIB}$, 6 mice (*, $p<0.05$, ***, $p<0.001$, #, $p>0.05$, all vs. the control group; two-way ANOVA; outliers that were larger than 2 standard deviations were excluded). i.t. injections were indicated by arrows.

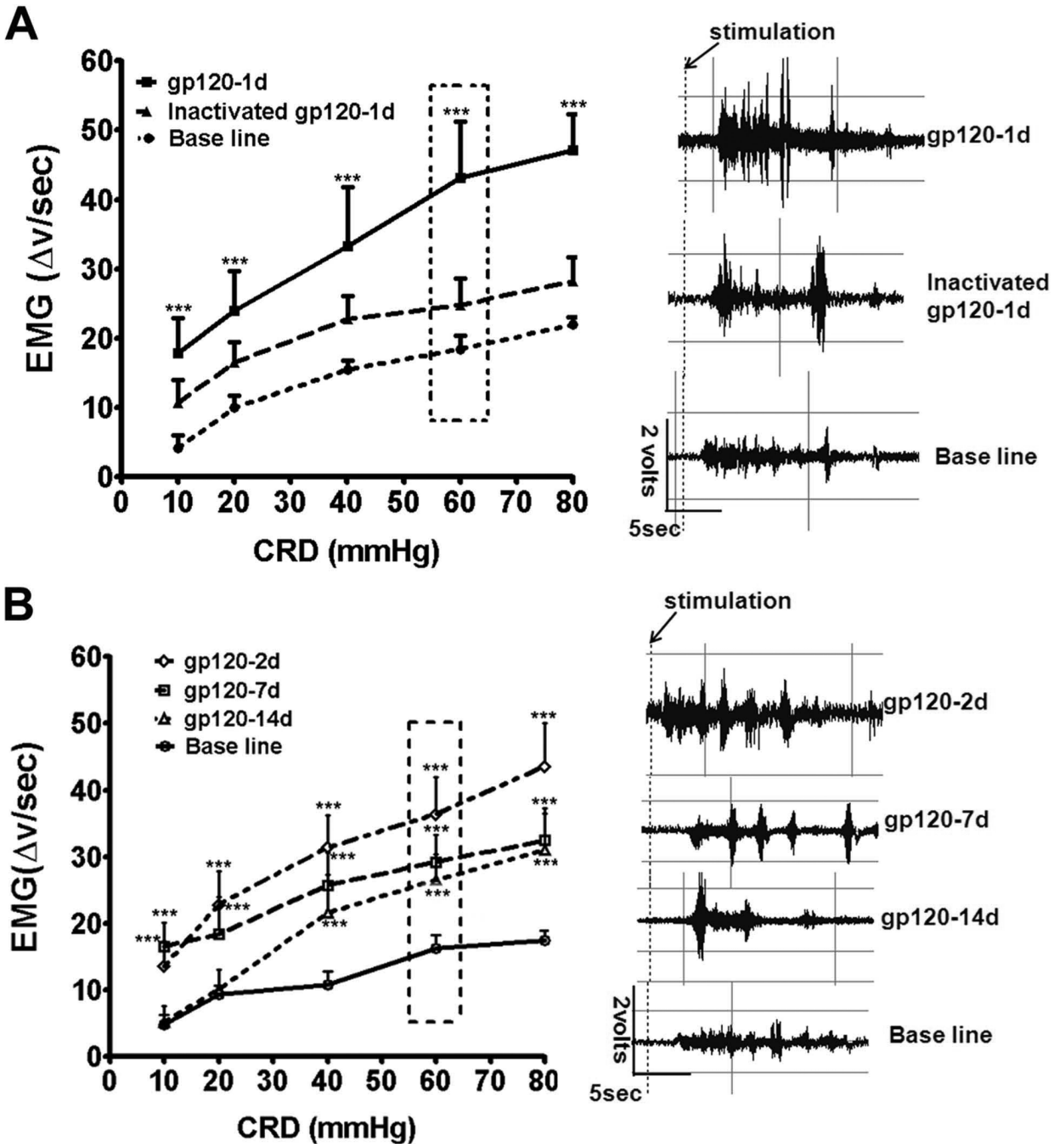

Figure 4.

i.t. gp120 caused visceral hyperalgesia in rats. A. Gp120 significantly increased electromyographic (EMG) activity induced by rectal distention at 24 hrs post i.t. injection (n = 6 rats, ***p<0.001, two way ANOVA vs. baseline). Heat-inactivated gp120 did not cause a significant increase of EMG activity. B. i.t. gp120-induced visceral hyperalgesia maintained on day 2, 7 and 14 post i.t. gp120 injection (n = 6, ***, p<0.001, two way ANOVA vs. baseline). Representative EMGs from the boxed distension pressure are shown to the right of each group.

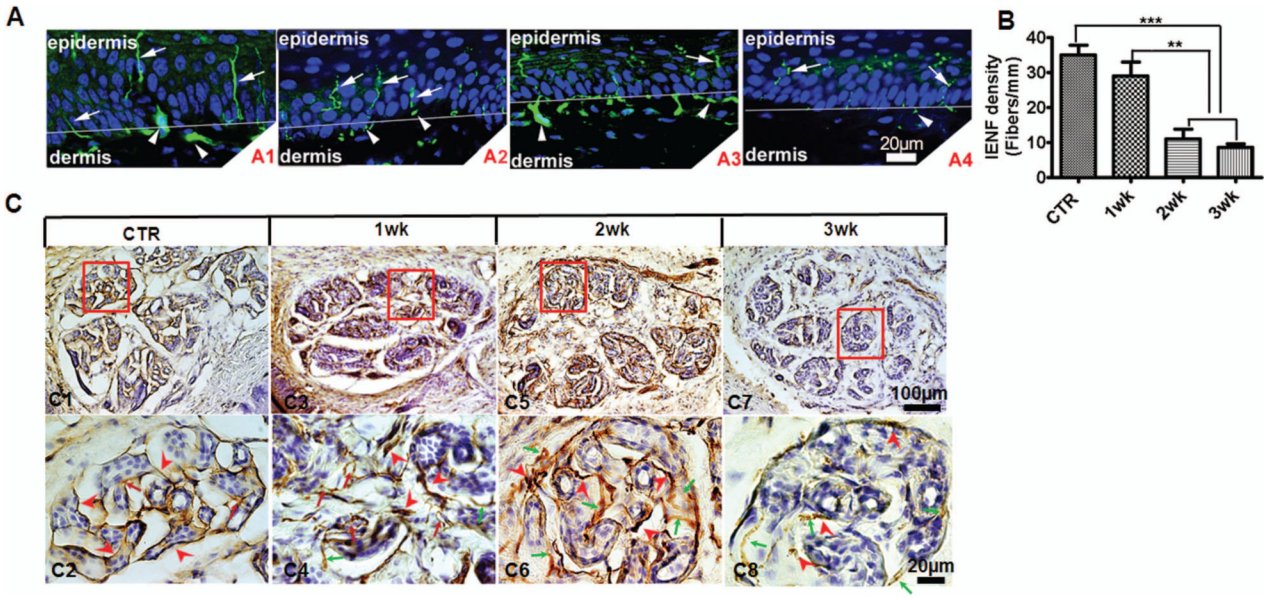

Figure 5.

i.t. gp120 caused peripheral neuropathy. To model chronic gp120 exposure in patients, gp120 was applied 3 times (days 0, 2 & 4). PGP9.5 staining is shown at 1, 2 and 3 weeks (wk) post the 1st i.t. control (CTR): i.t. of boiled gp120 did not cause a detectable effect. i.t. gp120 injections were performed following the paradigm indicated in Fig. 2B. A. Immunofluorescent images of PGP9.5-positive nerve fibers in the epidermis and dermis of plantar footpads of mouse hind paws. A1. Skin of control mice (i.t. boiled gp120). Smooth fibers innervating in the epidermis (arrows) and nerve bundles in the dermis (arrowheads) were clearly seen. DAPI staining: blue. A2. One week post 1st i.t. gp120 injection. Nerve fibers innervating in the epidermis were detected with swollen or fragmented regions (arrows). A3. Two weeks post 1st i.t. gp120. Prominent fragmentation of nerve fibers was seen in the epidermis (arrows). Nerves in the dermis also started to show swollen or fragmented regions (arrowheads). A4. Three weeks post 1st i.t. gp120. Reduced PGP9.5-positive fibers were seen in both epidermis and dermis. B. Intra-epidermal nerve fiber (IENF) density. Fibers with a clear morphology that crossed the dermis/epidermis junctions were counted (48 sections from 6 mice/group; ***, $p<0.001$; **, $p<0.01$; one-way ANOVA). C. Diaminobenzidine (DAB) staining PGP9.5-positive nerve fibers innervating in eccrine glands in the plantar hind paw. Low-magnification images: C1, C3, C5 and C7. Higher magnification of the boxed areas: C2, C4, C6 and C8. The plantar eccrine glands were normally innervated with fine and compact PGP9.5-positive fibers (red arrowheads) with a few branches (red arrows) in control mice (C1, C2). At 1-week post i.t. gp120 administration (as in A), dense and dark-stained innervating fibers were observed around the eccrine glands (C3, C4). Swollen fibers (red arrowheads) and more disorganized branches (red arrows) appeared. Some fibers began to degenerate (green arrows) (C4). At 2 weeks (C5 and C6), evident swelling (red arrowheads) and degeneration (green arrows) were seen (C6). At 3 weeks, PGP9.5-positive fibers were greatly reduced. Only few dark-stained fragments (red arrowheads) and degenerated fibers (green arrows) were seen (C7, C8).

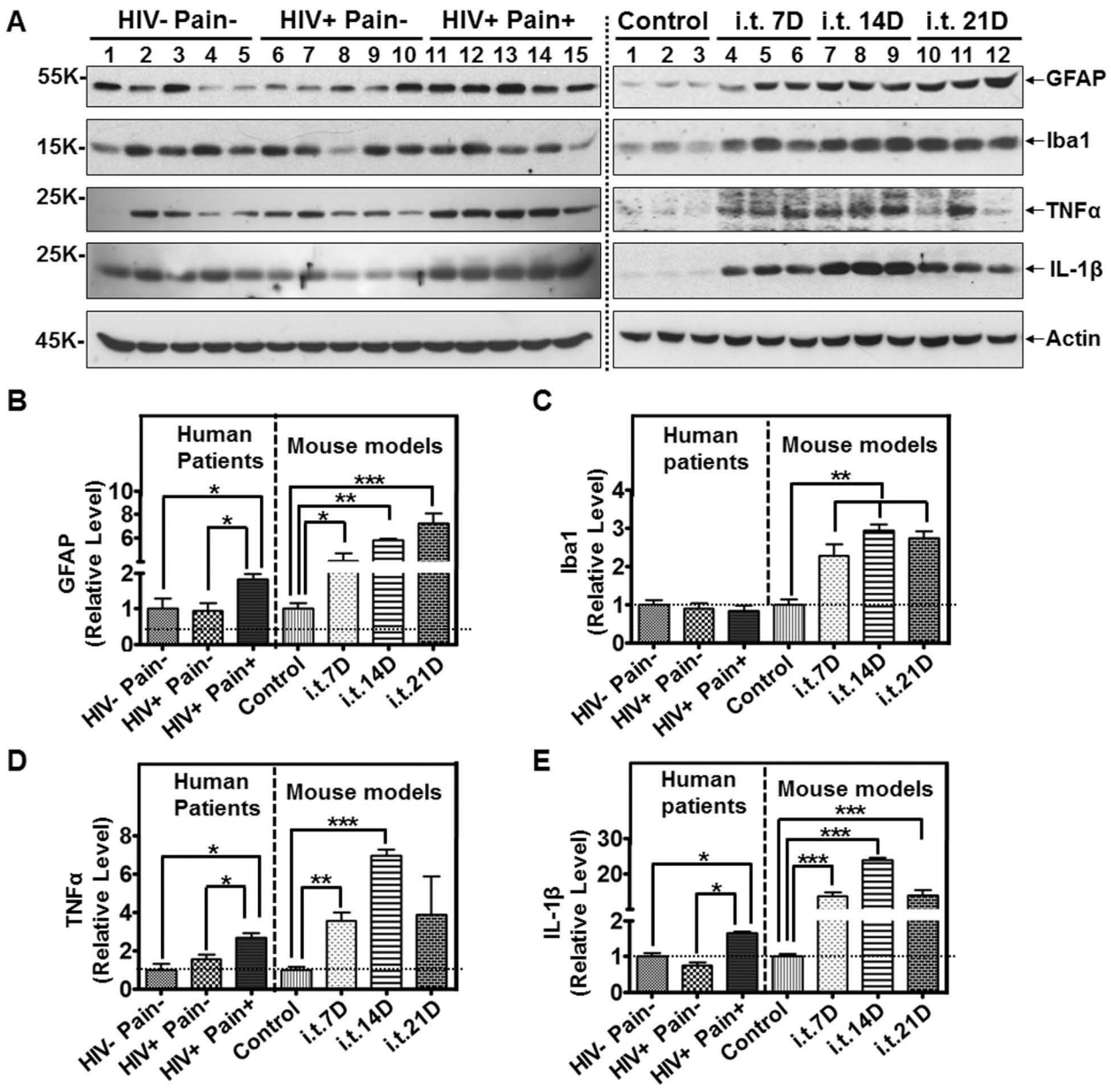

Figure 6.

Glial activation in the SDH of 'pain-positive' HIV-1 patients and i.t. gp120 mice. A. Immunoblots of GFAP, Iba1, TNFα and IL-1β in the SDH of human patients (left panel) and i.t. gp120 mice at day 7 (7D), 14D or 21D (right panel). GFAP was increased both in the 'pain-positive' HIV patients and i.t. gp120 mice. Iba1 was not increased in the 'pain-positive' HIV-1 patients but was up-regulated in the i.t. gp120 mice. TNFα and IL-1β were significantly increased in the 'pain-positive' HIV-1 patients and i.t. gp120 mice. B-E. Quantitative summary (human patient specimens: 5/group; mice: 6/group. The same sample sizes were used in Fig. 7 and Fig. 8) of GFAP (B), Iba1 (C), TNFα (D) and IL-1β (E). For mice used in this and subsequent figures, i.t. injection of gp120 was performed following the paradigm indicated in Fig. 3. (*, $p<0.05$; **, $p<0.01$; ***, $p<0.001$; One-way ANOVA).

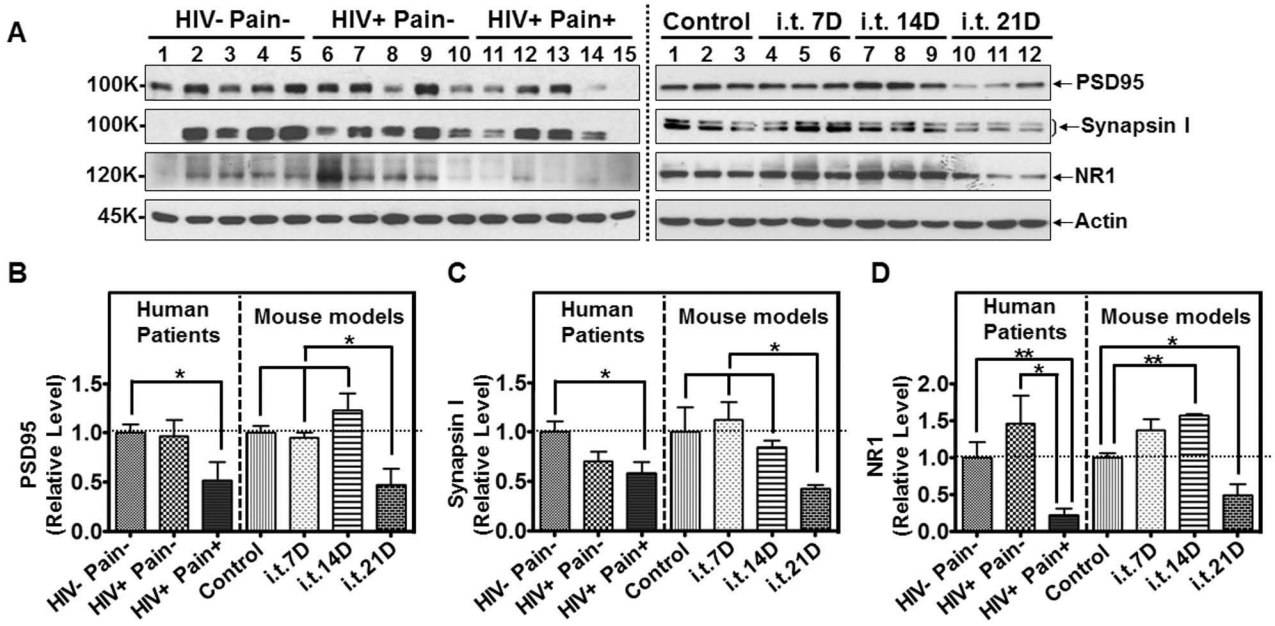

Figure 7.

Synaptic abnormalities in the SDH of 'pain-positive' HIV-1 patients and i.t. gp120 mice. A. Immunoblots of PSD95, Synapsin I and NR1 in the SDH of human patients (left panel) and i.t. gp120 mice at day 7 (7D), 14D or 21D (right panel). B-D. Quantitative summary of PSD95 (B), Synapsin I (C) and NR1 (D). (*, $p<0.05$; **, $p<0.01$; One-way ANOVA)

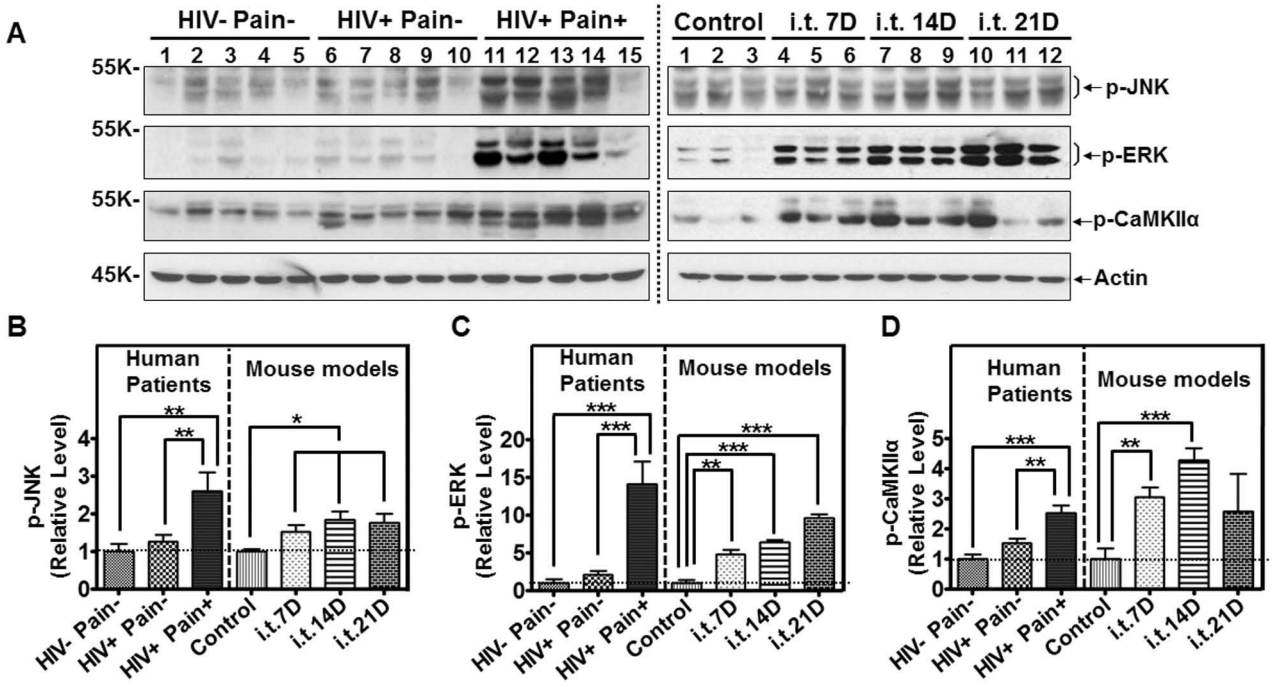

Figure 8.

Comparison of signaling pathways in the SDH of 'pain-positive' HIV-1 patients and i.t. gp120 mice. A. Immunoblots of phosphorylated JNK (p-JNK), phosphorylated ERK (p-ERK) and phosphorylated CaMKIIα (p-CaMKIIα) in the SDH of human patients (left panel) and i.t. gp120 mice at day 7 (7D), 14D or 21D (right panel). B-D. Quantitative summary of p-JNK (B), p-ERK (C), and p-CaMKIIα (D). (*, $p<0.05$; **, $p<0.01$; ***, $p<0.001$; One-way ANOVA)